J. Biochem. **139**, 715–723 (2006)
doi:10.1093/jb/mvj084

Binding Investigation of Human 5-Lipoxygenase with Its Inhibitors by SPR Technology Correlating with Molecular Docking Simulation

Li Du[1,*], Zhenshan Zhang[1,*], Xiaomin Luo[1], Kaixian Chen[1], Xu Shen[1,2,†] and Hualiang Jiang[1,2,†]

[1]Drug Discovery and Design Center, State Key Laboratory of Drug Research, Shanghai Institute of Materia Medica, Shanghai Institutes for Biological Sciences, Graduate School of the Chinese Academy of Sciences, Chinese Academy of Sciences, Shanghai 201203, China; and [2]School of Pharmacy, East China University of Science and Technology, Shanghai 200237, China

Received December 8, 2005; accepted February 9, 2006

The binding features of a series of 5-lipoxygenase (5-LOX) inhibitors (caffeic acid, NDGA, AA-861, CDC, esculetin, gossypol and phenidone) to human 5-LOX have been studied by using surface plasmon resonance biosensor (SPR) technology based Biacore 3000 and molecular docking simulation analyses. The SPR results showed that the equilibrium dissociation constant (K_D) values evaluated by Biacore 3000 for the inhibitors showed a good correlation with its reported IC_{50}, suggesting that SPR technology might be applicable as a direct assay method in screening new 5-LOX inhibitors at an early stage. In addition, the 3D structural model of 5-LOX was generated according to the crystal structure of rabbit reticulocyte 15-lipoxygenase, and the molecular docking simulation analyses revealed that the predicted binding free energies for the inhibitors correlated well with the K_D values measured by SPR assay, which implies the correctness of the constructed 3D structural model of 5-LOX. This current work has potential for application in structure-based 5-LOX inhibitor discovery.

Key words: arachidonic acid, 5-lipoxygenase inhibitors, molecular docking, surface plasmon resonance (SPR).

Abbreviations: 5-LOX, 5-lipoxygenase; SPR, surface plasmon resonance; K_D, equilibrium dissociation constant.

5-Lipoxygenase (5-LOX) belongs to a family of lipid peroxidising enzymes expressed in both the vegetal and the animal kingdoms (*1*). It catalyses the first two steps in leukotriene A_4 (LTA_4) biosynthesis: the oxidation of arachidonic acid (AA) at C-5 to yield 5-hydroxy-6,8,10,14-eicosatetraenoic acid (5-HPETE) (5-oxygenase activity), and the subsequent dehydration of this hydroperoxide to the key intermediate LTA_4 (LTA_4 synthase activity) (*2*), which is followed by the synthesis of leukotrienes (LTs) (*3*, *4*). LTA_4 is a potent chemotactic agent of inflammatory cells such as neutrophils, macrophages and eosinophils, and plays an important role in immune reactions by enhancing the release of pro-inflammatory cytokines from macrophages and lymphocytes (*5*). LTs are lipid messengers that play central roles in immune response and tissue homeostasis, and have been regarded as important mediators of numerous inflammatory diseases and allergic disorders such as rheumatoid arthritis, inflammatory bowel disease, ulcerative colitis, asthma, psoriasis and allergic rhinitis (*6*). Besides its important roles in inflammatory diseases, 5-LOX is also involved in the development and progression of numerous types of cancer such as pancreatic, lung, colorectal and prostate (*7*–*9*). Therefore, because of its potent biological activities in the synthesis of LTs, 5-LOX has been developed as an important therapeutic target in the treatment of various inflammatory diseases such as asthma, allergic and inflammatory disorders (*10*).

Research in different mammalian species has demonstrated that 5-LOX is a monomeric enzyme with estimated molecular mass of 75–80 kDa, containing about 673 amino acids (*11*, *12*). While the 3D structure of 5-LOX has not been determined yet, several crystal structures of LOXs have been reported: two isoforms from soybeans, LOX-1 and LOX-3, and 15-LOX from rabbit (*13*, *14*). Based on these crystallographic data, the LOX enzymes seem to share an overall folding pattern comprised of two distinct units: a small N-terminal β-barrel domain, and a larger C-terminal catalytic domain mainly composed of α-helices (*15*). Cellular 5-LOX activity is regulated by a complex mechanism that involves calcium ions, adenosine triphosphate, phosphorylation and gene transcription. Calcium ions bind to 5-LOX with an equilibrium dissociation constant (K_D) of 6 μM, increasing the hydrophobicity of 5-LOX and promoting membrane association (*16*).

In regard to the characteristics and mechanism of action for 5-LOX, different strategies have been developed to inhibit the 5-LOX pathway, and many 5-LOX inhibitors have been discovered, including redox inhibitors or antioxidants that interfere with the redox cycle of 5-LOX, and non-redox competitive inhibitors that compete with AA to bind to the enzyme active site. However, previous reports predominantly focused only on the effects of the inhibitors on

*These two authors contributed equally.
†To whom correspondence should be addressed. Tel/Fax: +86-21-50806918, E-mail: xshen@mail.shcnc.ac.cn (X. Shen); hljiang@mail.shcnc.ac.cn (H. Jiang).

the 5-LOX enzyme activity or LT biosynthesis (*17–20*). Few studies have presented the direct binding data of 5-LOX enzyme to the inhibitors, and details of their interactions remain obscure, which is a major obstacle to structure-based 5-LOX inhibitor discovery.

Recently, the surface plasmon resonance (SPR) biosensor has been successfully used to detect the interactions of small molecules with receptors (*21*). This powerful tool permits the investigation of macromolecule-ligand interactions in real time without the need for labelling. In the current work, SPR technology–based Biacore 3000 was successfully applied to determine the binding affinities of 5-LOX to its substrate AA and seven typical inhibitors, *viz*, CDC, esculetin, NDGA, gossypol, caffeic acid, phenidone and AA-861 (Scheme 1). The equilibrium dissociation constant (K_D) values evaluated by Biacore 3000 for the inhibitors demonstrated a good correlation with their reported IC_{50} values, which suggests that SPR technology could be developed as a direct assay method in screening new 5-LOX inhibitors at an early stage. To further investigate the 5-LOX/inhibitor binding mode at the atomic level, molecular docking was performed with the 3D structural model of 5-LOX generated on the basis of the crystal structure of rabbit reticulocyte 15-lipoxygenase (PDB entry code 1LOX). The predicted binding free energies for the inhibitors showed a good correlation with the K_D values measured by SPR assay, implying the correctness of our constructed 3D structural model of 5-LOX. The molecular docking technology in this work has thus provided a reasonable and reliable 5-LOX/inhibitor binding model, which has potential for application in the structure-based discovery of novel 5-LOX inhibitors.

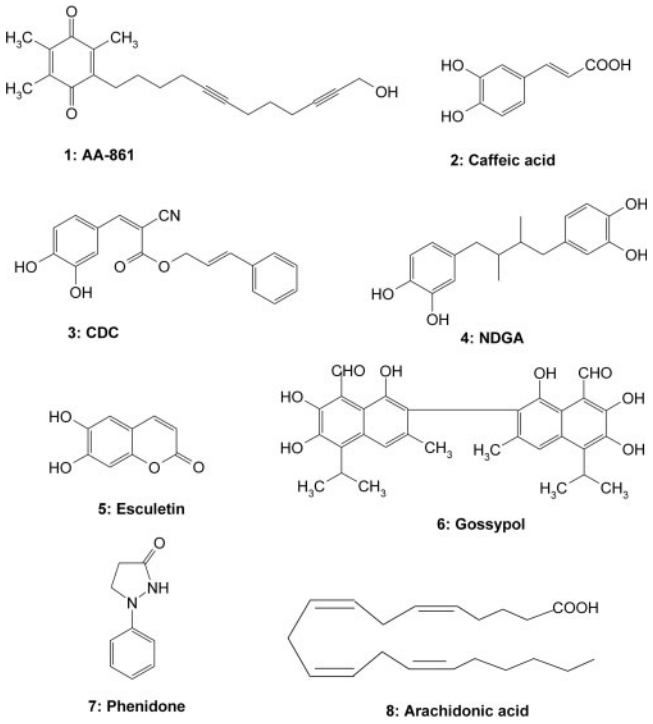

Scheme 1. **Structures of the seven tested inhibitors of 5-LOX and its substrate arachidonic acid.**

MATERIALS AND METHODS

Cells and Cell Culture—Trichoplusia ni (TN) insect cells were obtained from the Cell Bank in the Institute of Cell Biology (Shanghai, China) and routinely grown in Grace's Insect Cell Culture Medium (Gibco) with 10% heat-inactivated fetal bovine serum at 28°C.

Chemicals and Reagents—Caffeic acid and NDGA were purchased from Cayman Chemical Company. AA-861, CDC, esculetin, gossypol and phenidone were purchased from Biomol Co. The structures of the seven studied 5-LOX inhibitors are shown in Scheme 1. All of the tested compounds were dissolved in dimethyl sulfoxide (Me_2SO) as 10 mM stock solution for use.

The Gibco BRL BAC-To-BAC Baculovirus Expression System, which includes pFastBac donor plasmid, MAX efficiency DH_{10}Bac competent cells and cellfectin reagent, was a gift from Professor Q. F. Wu (Shanghai Institute of Biological Science, Chinese Academy of Sciences, China). Grace's Insect Cell Culture Medium and Sf-900 II SFM insect cell culture medium were purchased from Gibco and Invitrogen. Fetal bovine serum was obtained from Hyclone.

All the other reagents were purchased from Sigma.

Expression of 5-LOX by Recombinant Baculovirus in Insect Cells—The plasmid pT3-5LOX, which contains the cDNA sequence of human 5-lipoxygenase, was generously donated by Professor Olof Radmark (Department of Medical Biochemistry and Biophysics, Division of Physiological Chemistry II, Karolinska Institute, Sweden). The 2,025-base pair fragment was subcloned into the *Eco*RI and *Sal*I sites of a pFastBac donor plasmid, pFastBacHTa, to generate pFastBacHTa-5LOX. The pFastBacHTa-5LOX was transfected into DH_{10}Bac competent cells to get the recombinant Bacmid DNA. The recombinant Bacmid DNA was then transfected into *Trichoplusia ni* (TN) insect cells along with cellfectin reagent to generate recombinant virus (5-LOX virus stock) according to the Instruction Manual of the Gibco BRL BAC-To-BAC Baculovirus Expression System. 5-LOX virus was harvested 2 days post-transfection and titered as described in the Instruction Manual. TN cells were grown in Grace's Insect Cell Culture Medium (GIBCO) with 10% heat-inactivated fetal bovine serum and 1× penicillin/gentamicin to ~9.0 × 105 cells/ml were infected with 5-LOX virus stock at a multiplicity of infection 4. After 72 h, the infected cells were harvested by centrifugation for 20 min at 5,000 rpm, 4°C and immediately stored at –80°C.

Purification of the Recombinant Baculovirus-Expressed 5-LOX—The 5-LOX virus–infected cells were resuspended in 20 ml of buffer A (20 mM Tris-HCl, 500 mM NaCl, 5mM imidazole) and lysed by sonication for 10 min in an ice bath. The lysate was centrifuged for 30 min at 15,000 rpm, 4°C. The supernatant was loaded on a 3-ml Sepharose Ni-NTA column (Novagen) equilibrated with 30 ml of buffer A. The column was then washed with 15 ml of buffer B (20 mM Tris-HCl, 500 mM NaCl, 50 mM imidazole) and eluted with buffer C (20 mM Tris-HCl, 500 mM NaCl, 100 mM imidazole). The eluted fraction was dialysed to buffer D (10 mM HEPES and 150 mM NaCl) and concentrated by Centricon (Millipore). The purity of the enzyme was determined by SDS-PAGE, and the concentration was monitored by

measuring the absorbance at 280 nm in buffer D using the extinction coefficent of 128,825 l/mol/cm.

5-LOX Enzyme Activity Assay—The assay mixture (1 ml) containing 160 μM arachidonic acid (AA), 1 mM ATP, 5 mM $CaCl_2$, 50 mM Tris-HCl (pH 7.5), 10 μM purified 5-LOX and 20 μg/ml phosphatidyl choline vesicles was incubated at room temperature for 15 min, and the reaction was stopped by addition of stop solution A [MeCN/MeOH/HOAc (1:1:0.002, v/v)]. The mixture was centrifuged at 15,000 rpm for 10 min, and an aliquot of the supernatant was injected on a Nova-Pak C18 HPLC column. The eluent was monitored at 234 nm to detect 5-HPETE and 5-HETE production (*22*).

Immobilization of the Recombinant 5-LOX on CM5 Sensor Chip Surface—The binding of the 5-LOX enzyme and its inhibitors was analyzed using the dual flow cell Biocore 3000 instrument (Biocore AB, Uppsala, Sweden) with 5-LOX enzyme immobilized on the Biacore CM5 sensor chip. Immobilization of the enzyme to the hydrophilic carboxymethylated dextran matrix of the sensor chip was carried out by the standard primary amine coupling method, and the resonance signal reached about 10,000 resonance units (RUs). The enzyme to be covalently bound to the matrix was diluted in 10 mM sodium acetate buffer (pH 4.2) to a final concentration of 0.2 mg/ml. Equilibration of the baseline was completed by passing a continuous flow of HBS-EP buffer (10 mM HEPES, 150 mM NaCl, 3 mM EDTA and 0.01% P20, pH 7.4) through the chip for 4–5 h.

SPR Technology–Based 5-LOX/Small Molecule Binding Assay—During the SPR experiments, the stock solutions of the 5-LOX substrate arachidonic acid (AA) and its inhibitors were diluted into the running buffer to make samples in a concentration range of 1–10 μM. All the sensorgrams were processed by using automatic correction for nonspecific bulk refractive index effects. The specific binding profiles of the ligands to the immobilized 5-LOX were obtained after subtracting the response signal from the control flow cell. All the Biacore data were collected at 25°C with HBS-EP as running buffer at a constant flow of 30 μl/min.

All the equilibrium dissociation constants (K_Ds) used for evaluating the enzyme-ligand binding affinity were determined with Biacore evaluation Version 3.0 software (Biacore). For each trial, the signal was corrected against the control surface response to eliminate any refractive index changes due to buffer change.

SPR Data Analysis—During the binding assays of 5-LOX and its inhibitors with Biacore 3000, the binding response signals in RUs were continuously recorded and presented graphically as a function of time. The association could be described in a simple equilibrium $A + B \rightleftharpoons AB$ (A, analyte; B, ligand; AB, complex formed by A and B). To determine the equilibrium dissociation constant (K_D) for the interaction, the equilibrium data were fitted to an independent-binding-site model (Eq. 1),

$$R_{eq} = \sum_i \frac{R_{max,j} \times C \times K_{on,i}}{1 + C \times K_{on,i}} \quad (1)$$

where, R_{max} stands for the maximal response, C is the concentration of a ligand, and K_{on} is the equilibrium association constant. For a single-site interaction, $i = 1$, for a two-site binding, $i = 2$, and so on. The Biacore results indicated that, in reaching equilibrium, both the association with and dissociation from the immobilized 5-LOX of the substrate arachidonic acid (AA) and the compounds caffeic acid, CDC, esculetin, AA-861, NDGA and gossypol involved slow phases as shown in Fig. 1 and Fig. 2A (using gossypol as a typical example). For phenidone, however, the association and dissociation phases were momentary, and the response reached the equilibrium quickly as reflected in Fig. 2B. Therefore, in the Biacore data analysis, two different fitting models were adopted. One is the 1:1 (Langmuir) binding fitting model, in which the association (k_{on}) and dissociation (k_{off}) constants are fitted simultaneously using Eq. 2:

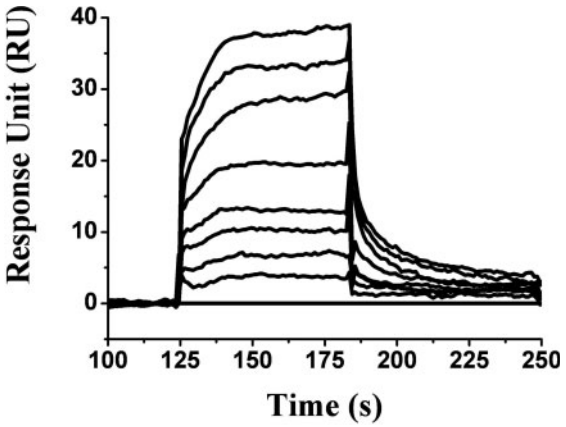

Fig. 1. **Kinetic analysis of the substrate arachidonic acid (AA) binding to 5-LOX by SPR technology–based Biacore 3000.** Representative sensorgrams obtained from injection of AA at concentrations of 0, 0.309, 0.441, 0.630, 0.900, 1.29, 1.84, 2.63 and 3.75 mM.

$$\frac{dR}{dt} = k_{on} \times C \times (R_{max} - R) - k_{off} \times R \quad (2)$$

where R represents the response unit, C is the concentration of the compound. For the compounds that reach the equilibrium slowly, both the association and dissociation phases were fitted simultaneously by using the 1:1 binding model (Langmuir) (*23*). The other is the steady-state affinity model, which was employed to calculate the binding affinities. Therefore, the binding kinetic constants of the tested inhibitors CDC, esculetin, NDGA, gossypol, AA-861 and caffeic acid, and the substrate AA could be calculated using Eq. 2, while the binding affinity (K_D) of phenidone to 5-LOX could be obtained by the steady-state affinity model. The steady state plots against the concentrations are shown in Fig. 3. The curve fitting efficiency was evaluated by residual plots and χ^2. All the results are summarized in Tables 1 and 2.

Molecular Modeling—The 3D structures of the inhibitors used in the study were constructed using the standard geometric parameters of molecular modeling software package SYBYL 6.8 (*24*) based on the Tripos force field (*25*) and Gasteiger-Huckel charge (*26*, *27*). Geometric optimizations were performed by Powell first and then conjugate gradient procedures with a 0.05 kcal·mol^{-1} Å^{-1} energy gradient convergence criterion and a distance-dependent

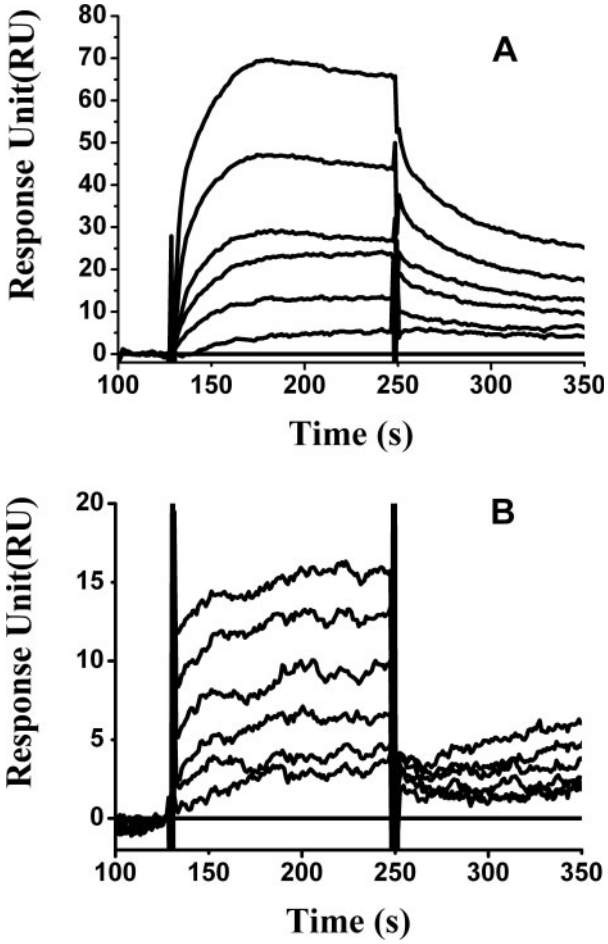

Fig. 2. **Kinetic analyses of Gossypol and Phenidone binding to 5-LOX.** Representative sensorgrams obtained from injections of Gossypol at concentrations of 0, 1.6807, 2.401, 3.43, 4.9, 7.0, and 10 μM (A); and Phenidone at concentrations of 0, 1.6807, 2.401, 3.43, 4.9, 7.0, and 10 μM (B).

dielectric constant. The sequence of the 674 animo acids of human 5-LOX was obtained from the Swissprot database (http://us.expasy.org/sprot/). Sequence analysis and structurally conserved region determination were performed for soybean lipoxygenases and rabbit 15-lipoxygenase. The 3D structural model of 5-LOX was generated using the automated homology modeling program Modeller (*28*) based on the crystal structure of rabbit reticulocyte 15-lipoxygenase (PDB entry code 1LOX). The modeled 5-LOX was subjected to energy optimization with conjugate gradient minimization followed by a medium simulated annealing molecular dynamics scheme. The final model protein was validated by both Profiles 3D and Procheck (*29*, *30*).

Molecular Docking—The putative binding pocket was determined according to the published results of site-mutagenesis and complex structures, which is mainly composed of the conserved residues of His 368, Leu 369, Ile407, Leu 415, Leu 608 and Ile 674 (*14*, *15*, *22*, *31*). The metal ion Fe(II), which is supposed to form five coordinated bonds with the enzyme (Fig. 5A), was taken into account during the docking calculation for its key role in both substrate binding and catalysis. The seven tested inhibitors, caffeic acid, NDGA, AA-861, CDC, esculetin, gossypol and

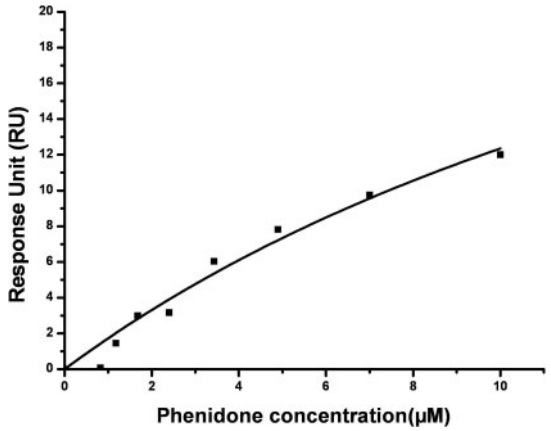

Fig. 3. **Equilibrium data analysis of Phenidone binding to 5-LOX.** The data for the SPR sensorgrams were fitted to a single-site interaction model. The plots of steady state RU *vs.* Phenidone concentrations were obtained by using a steady-state fitting model.

phenidone, were docked into the binding site of the enzyme employing the flexible docking program AutoDock 3.0.3 (*32*). For the docking simulations, the standard parameters of the AutoDock 3.0.3 were used, and the configuration of the compounds corresponding to the lowest binding free energy was chosen for further analysis of the correlation between the binding free energy and the inhibitory activity. AutoDock 3.0.3 was used to calculate the binding free energy between ligand and receptor and estimate K_i value through its empirically calibrated score function. This new score function computes not only the restriction of the global rotation, internal rotors, and the translation, but also the desolvation upon binding and the hydrophobic effect. Accordingly, the scoring function could measure the ligand-enzyme binding free energy more accurately.

All Molecular Modeling and Docking Simulations Were Carried Out on a Four-CPU Silicon Graphic Origin3200 Workstation.

RESULTS

SPR-Based Binding Assay between Arachidonic Acid (AA) and the Immobilized Recombinant 5-LOX—To investigate the interaction of the substrate arachidonic acid (AA) with the immobilized recombinant 5-LOX on the CM5 sensor chip, AA was diluted into the running buffer at concentrations ranging from 0.3 to 5 mM. As shown in Fig. 1, the RU values evaluating the AA binding to the immobilized 5-LOX revealed an obvious concentration-dependent manner, and the binding kinetic constants were fitted using the 1:1 (Langmuir) binding fitting model supplied in the Biacore software. The results are listed in Table 1, which demonstrated that the determined equilibrium dissociation constant (K_D) of 3.51 ± 0.126 mM is close to the K_m value of 3.8 mM for 5-LOX against arachidonic acid (*33*). Since the K_m value reflects the enzyme's binding capacity to the substrate, the closely comparable value of the binding affinity (K_D) measured by Biacore 3000 with the K_m value indicated that the immobilized 5-LOX was completely active, and SPR technology could be a reliable tool for investigating the interactions between 5-LOX and its ligands.

Table 1. **Kinetic parameters of the binding of arachidonic acid (AA) to 5-LOX.**

R_{max} (RU)	k_{on} (M^{-1} s^{-1})	k_{off} (s^{-1})	K_D (M)	χ^2
37.2 ± 2.16	10.2 ± 0.745	0.0359 ± 0.000976	$3.51 \pm 0.126 \times 10^{-3}$	0.492

R_{max}, maximum analyte binding capacity; k_{on}, association rate constant; k_{off}, dissociation rate constant; K_D, equilibrium dissociation constant. $K_D = k_{off}/k_{on}$; χ^2, statistical value in Biacore.

Table 2. **Kinetic parameters of the binding of inhibitors to 5-LOX.**

Compound	k_{on} (M^{-1} s^{-1})	k_{off} (s^{-1})	K_D (M)	χ^2
CDC	$5.24 \pm 0.105 \times 10^3$	$5.58 \pm 0.0618 \times 10^{-3}$	$1.07 \pm 0.0524 \times 10^{-6}$	6.53
Esculetin	$3.76 \pm 0.0827 \times 10^3$	$8.35 \pm 0.203 \times 10^{-3}$	$2.22 \pm 0.101 \times 10^{-6}$	0.399
NDGA	166 ± 1.52	$3.73 \pm 0.121 \times 10^{-5}$	$2.25 \pm 0.125 \times 10^{-7}$	0.749
Gossypol	$1.39 \pm 0.111 \times 10^3$	$3.23 \pm 0.0867 \times 10^{-3}$	$2.33 \pm 0.0932 \times 10^{-6}$	3.26
AA-861	35.5 ± 3.27	$1.79 \pm 0.103 \times 10^{-5}$	$5.04 \pm 0.426 \times 10^{-7}$	0.470
Caffeic acid	$7.31 \pm 0.540 \times 10^3$	0.0554 ± 0.00318	$7.57 \pm 0.0642 \times 10^{-6}$	0.177

k_{on}, association rate constant; k_{off}, dissociation rate constant; K_D, equilibrium dissociation constant. $K_D = k_{off}/k_{on}$; $\chi 2$, statistical value in Biacore.

Table 3. **Equilibrium dissociation constant (K_D) values determined by SPR assay and the reported IC_{50} values.**

Compound	K_D in this study (μM)	IC_{50} in reference (μM)
CDC	1.07 ± 0.0524	1.87[a]
Esculetin	2.09 ± 0.101	4.00[b]
AA-861	0.504 ± 0.0426	0.8[c]
Caffeic acid	7.57 ± 0.0642	3.7[d]
Phenidone	21.5 ± 1.87	24[e]
NDGA	0.225 ± 0.0125	0.2[f]
Gossypol	2.33 ± 0.0932	0.3[g]

[a]Ref. *34*; [b]Ref. *35*; [c]Ref. *36*; [d]Ref. *37*; [e]Ref. *38*; [f]Ref. *39*; [g]Ref. *40*.

Correlation of Binding Affinities and Inhibitory Activities—Shown in Table 3 are the K_D and IC_{50} values of all the seven tested 5-LOX inhibitors. The K_D values of the inhibitors binding to 5-LOX were generally in good agreement with their IC_{50} values. For CDC, esculetin, AA-861, caffeic acid, phenidone and NDGA, their K_D values are nearly within the same quantitative grade compared with the reported IC_{50} values (*34–39*), although for gossypol, its K_D value is slightly higher than its reported IC_{50} value (*40*).

Binding Models—To address the structure-binding affinity relationship and explore the binding characteristics of the inhibitors to 5-LOX at the molecular level, the binding models of the tested inhibitors with 5-LOX were constructed.

The 3D structural model of 5-LOX was based on the crystal structure of rabbit reticulocyte 15-lipoxygenase (PDB entry code 1LOX). The sequence alignment between the two proteins calculated by CLUSTALW (*41*) indicates that the sequence identity between them is 42.35% (Fig. 4). This high identity value supports the models' reliability.

The 3D binding modes of the ligands to 5-LOX are schematically illustrated in Fig. 5 based on the ligands' conformation corresponding to the lowest binding free energies calculated by AutoDock 3.0.3. The hydrogen bonds and hydrophobic interactions were calculated by HBPLUS (*42*) and LIGPLOT (*43*) programs, respectively.

Compounds AA-861, caffeic acid and phenidone were used as three examples to elucidate the possible characteristics of the binding modes and inhibitory mechanisms for the inhibitors against 5-LOX. As shown in Fig. 5B, the binding mode between AA-861 and 5-LOX reveals a typical inhibitory mechanism of a good inhibitor for 5-LOX, which should have a polar head and tail, with a hydrophobic body. The carbonyl oxygen atom in the polar head of trimethyl *p*-benzoquinone of AA-861 forms a hydrogen bond with the N atom at the backbone of Ser 609, and its polar tail hydroxyl forms another strong hydrogen bond with the ND1 atom in the side chain of His 368. The two hydrogen bonds should greatly determine the orientation of AA-861 in the binding site and stabilize the hydrophobic interactions of the inhibitor's lathy hydrophobic body with the side chains of residues Leu 369, Ile 407, Ala 425, Leu 421, and Ile 674, *etc.* The binding mode of caffeic acid with 5-LOX is shown in Fig. 5C. There are two hydrogen bonds between the two hydroxyls in the polar head of pyrocatechol of caffeic acid and the protein: one hydrogen bond is with the NE2 atom in the side chain of Gln 558, the other is with the OG atom in the side chain of Ser 609. A third hydrogen bond is formed between the carboxyl in the polar tail of caffeic acid and the oxygen atom in the main chain of Gln 364. Because of its shorter hydrophobic body, the hydrophobic interactions are obviously reduced compared with that of AA-861, which might account for the decrease of the inhibitory activity of caffeic acid. Figure 5D depicts the binding mode of phenidone with 5-LOX. This compound has hydrophobic interactions with the protein through its non-polar head, phenyl, with residues Ile 407, Ile 674 and Leu 608. The weak electrostatic interactions might be generated between its polar tail pyrazolidinyl and polar side chains of residues Gln 364 and His 368. Without the hydrophobic body, its binding affinity with 5-LOX is poor (Table 4).

Generally, the binding modes of these inhibitors to 5-LOX are analogous: the polar head and tail interact with the hydrophilic portion of 5-LOX through hydrogen bonds or electrostatic interactions, and the hydrophobic body stretches into the large hydrophobic channel of 5-LOX to form strong hydrophobic interactions with its surrounding lipophilic residues. These could be viewed as the structural requirements for a 5-LOX inhibitor.

Correlation of Binding Free Energies with Binding Affinities and Inhibitory Activities—The binding energy could be regarded as an index of binding affinity

```
1-LOX     LYC-QQYLAAPLVMLKLQPDGKLMPMVIQLHLPKIGSSPPPLFLPTDPPMVWLLAKCWVR 348
5-LOX     DPCTLQFLAAPICLLYKNLANKIVPIAIQLN--QIPGDENPIFLPSDAKYDWLLAKIWVR 356
            *  *:****: :*  :  .*::*:.***: .:* ..  *:***:*.   ***** ***

1-LOX     SSDFQVHELNSHLLRGHLMAEVFTVATMRCLPSIHPVFKLIVPHLRYTLEINVRARNGLV 408
5-LOX     SSDFHVHQTITHLLRTHLVSEVFGIAMYRQLPAVHPIFKLLVAHVRFTIAINTKAREQLI 416
          ****:**:  :**** **::*** :*  * **::**:***:*.*:*:*: **.:**: *:

1-LOX     SDFGIFDQIMSTGGGGHVQLLQQAGAFLTYRSFCPPDDLADRGLLGVESS---FYAQDAL 465
5-LOX     CECGLFDKANATGGGGHVQMVQRAMKDLTYASLCFPEAIKARGMESKEDIPYYFYRDDGL 476
          .: *:**:  :********::*:*   *** *:* *: :  **: . *.    ** :*.*
```

Fig. 4. **Sequence alignments of rabbit reticulocyte 15-lipoxygenase (PDB entry code 1LOX) with the 5-LOX generated by CLUSTALW.** In the sequences, an asterisk indicates an identical or conserved residue, a colon indicates a conserved substitution, a dot indicates a semi-conserved substitution.

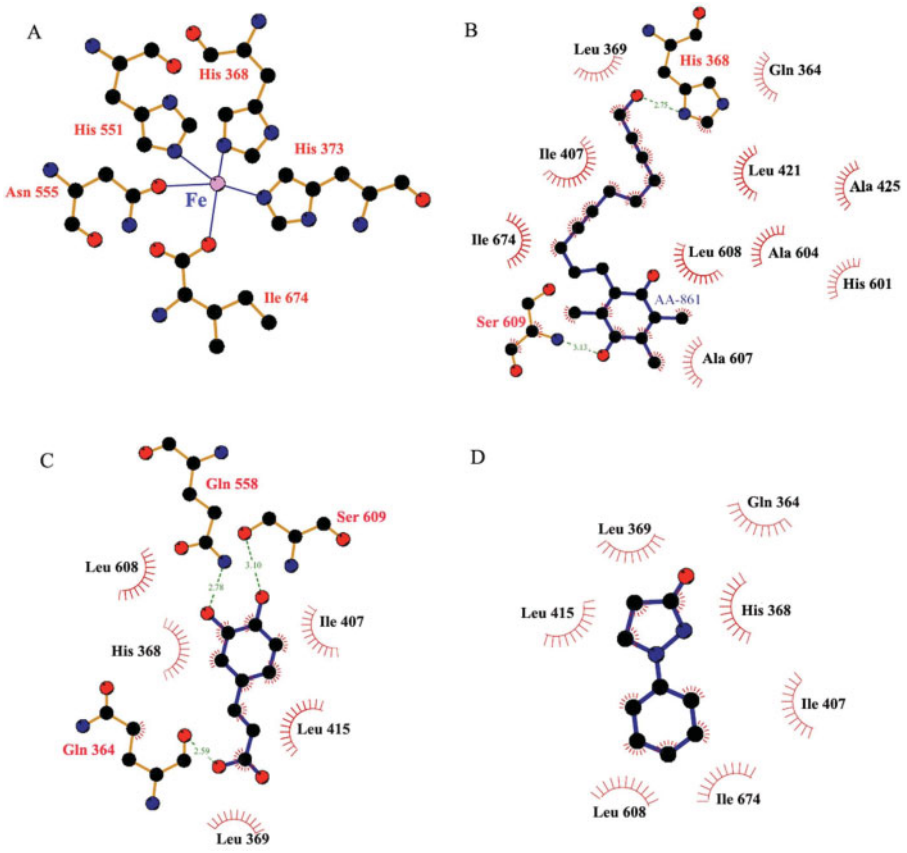

Fig. 5. **Schematic representations of hydrogen bonds and hydrophobic interactions of 5-LOX with metal Fe(II) ion (through coordinated bonds) (A), AA-861 (B), caffeic acid (C), and phenidone (D).** The hydrogen bonds and hydrophobic interactions were calculated by HBPLUS and LIGPLOT programs, respectively. Dashed lines represent hydrogen bonds, and spiked residues form hydrophobic contacts with the ligands.

(or inhibitory activity) of these inhibitors. Table 4 lists the binding free energies of the seven inhibitors to 5-LOX calculated by AutoDock 3.0.3. By means of a linear regression analysis, the regression equations for binding affinity (K_D) and inhibitory activity (IC_{50}) were respectively established by using the predicted binding free energy as the sole descriptor. It was demonstrated that the binding free energy exhibited good correlation with the SPR-determined K_D and reported IC_{50} shown by the following equations (Eqs. 3 and 4):

$$-\log K_D = -0.20 - 0.79 \times \Delta G_{binding} \quad (3)$$

$$n = 7, \text{SD} = 0.319, R^2 = 0.814$$

$$-\log IC_{50} = -0.17 - 0.80 \times \Delta G_{binding} \quad (4)$$

$$n = 6, \text{SD} = 0.411, R^2 = 0.728$$

where, n is the number of inhibitors, SD is the standard error, and R^2 is the correlation coefficient. Figures 6 and 7 depict the close correlation of the seven inhibitors' binding free energies with $-\log K_D$ and $-\log IC_{50}$ respectively, which further indicates the reliability of the binding conformations and binding modes derived from the docking simulation. Moreover, the predicted K_i values provided by AutoDock 3.0.3 of these inhibitors listed in Table 4 are basically proportional to the corresponding IC_{50} values, which also increase the credibility of the molecular modeling.

DISCUSSION

5-LOX, an important enzyme involved in the LTs synthesis pathway, has aroused considerable interest and been

Table 4. **Binding free energies and the estimated K_i, K_D and IC_{50} values of the binding of inhibitors to 5-LOX.**

Compound	Binding free energy (kcal/mol)[a]	Estimated K_i (μM)[b]	–log (IC_{50})[c]	–log (K_D)[d]
CDC	7.79	1.93	5.73	5.97
Esculetin	–7.3	4.45	5.40	5.68
AA-861	–8.21	0.955	6.10	6.30
Caffeic acid	–7.21	4.71	5.43	5.12
Phenidone	–5.9	7.53	4.62	4.67
NDGA	–8.02	1.33	6.70	6.65
Gossypol	–7.64	5.18	6.52	5.63

[a]The binding free energy (kcal/mol) was calculated by AutoDock 3.0.3; bestimated K_i was calculated by the following equation: $\Delta G = -RT\ln(1/K_i)$; [c]K_D values were measured by SPR; [d]IC_{50} values were from references.

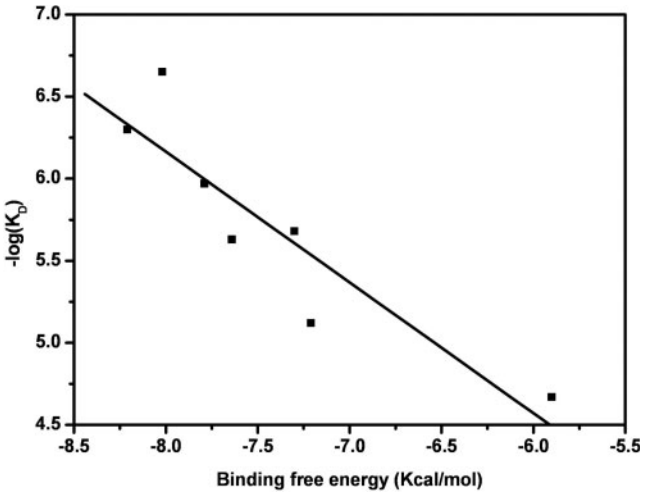

Fig. 6. **Correlation between SPR binding affinities and the Auto-Dock–predicted binding free energies.** The negative logarithm of K_D was plotted against the Auto-Dock–predicted binding free energies. The data were analysed by linear fitting method using Origin 6.1.

developed as a major target for the discovery of anti-inflammatory agents. Although various 5-LOX inhibitors have been synthesized or discovered to date, the direct mechanism by which they interact with 5-LOX is poorly understood due to the deficiency of structural information about 5-LOX.

In our study, for the first time, the binding interactions of 5-LOX with its inhibitors were directly measured by using the SPR biosensor technology. Because there are no reports on the K_D values for binding of the tested compounds to human 5-LOX, we compared of the K_D values obtained from the SPR assay and IC_{50} values in the previous references. Although the IC_{50} values of the tested inhibitors do not have an absolute relationship with their binding affinities (K_Ds) (Table 2), the positive correlation of the K_D and IC_{50} values might confirm the reliability of the SPR assay in the evaluation of 5-LOX interacting with its ligands, and SPR technology based Biacore 3000 could be used a useful tool in the discovery of 5-LOX inhibitors at an early stage. It is noticed that the K_D value of 2.33 μM for gossypol was slightly larger than its reported IC_{50} of 0.3 μM. Such an inconsistency might be due to the different experimental

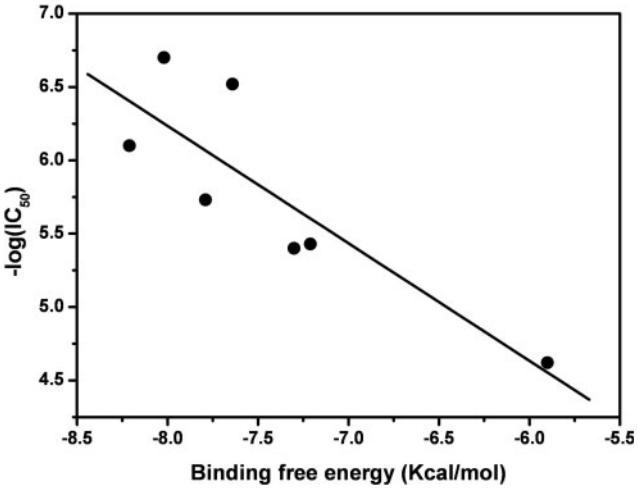

Fig. 7. **Correlation between inhibitory activity and the Auto-Dock–predicted binding free energies.** The negative logarithm of IC_{50} values was plotted against the Auto-Dock–predicted binding free energies. The data were analysed by linear fitting method using Origin 6.1.

conditions used in SPR assay and rat basophilic leukaemia cells (RBL-1) experiment (*40*).

Interestingly, it was also found that Ca^{2+} did not affect the binding affinities of the substrate AA and the tested inhibitors against 5-LOX during the Biacore assay, although some reports have stated that 5-LOX could be activated by Ca^{2+}, and Ca^{2+} binds to 5-LOX in a reversible manner (*44*). In this work, during the SPR assay, HBS-EP buffers containing added Ca^{2+} concentrations ranging from 0 to 20 mM were used as the running buffer for the kinetic analysis, but no changes in K_D were detected. This might because Ca^{2+} might affect mainly the oxidative activity and cellular localization of 5-LOX but have no impact on its structure or conformation (*45*, *46*). Since SPR associates with only the structure of the analyte and ligand, it is reasonable to assume that the Biacore assay could not detect the influence of Ca^{2+} on the binding ability of 5-LOX to its inhibitor or substrate.

To explore the binding characteristics of the inhibitors to 5-LOX at the molecular level, molecular docking was applied to construct the inhibitor/5-LOX binding model. As shown in Table 4 and Fig 6, the binding free energies predicted by docking are in good agreement with the K_D values obtained in SPR experiments, and the correlation coefficient (R^2) is as high as 0.814. Molecular docking results thus depict a general mode of binding of the inhibitors to 5-LOX. The inhibitors share some analogous features: a polar head and tail interacting with the hydrophilic portion of 5-LOX through hydrogen bonds or electrostatic interactions, and a hydrophobic body stretching into the large hydrophobic channel of 5-LOX to form strong hydrophobic interactions with its surrounding lipophilic residues. Shown in Fig 5 are schematic representations of three typical 5-LOX inhibitors interacting with 5-LOX, which revealed that hydrogen bonds and hydrophobic interaction might play a key role in inhibitor-enzyme binding. The abilities of the polar head and tail to form hydrogen bonds and of the body to form hydrophobic interactions with 5-LOX determine the inhibitor's

binding affinity. This explains adequately why phenidone, an inhibitor without a hydrophobic body, is the weakest 5-LOX binder.

As has been mentioned, SPR technology has been recognized as a powerful tool for investigating the interactions between macromolecules and small molecules with the advantages of permitting real-time measurement without the need for labeling. In traditional screening of 5-LOX inhibitors, whole human blood was usually used for monitoring the 5-LOX reaction products—LTB_4 and LTC_4 by radioimmunoassay (RIA) (*47*, *48*), or rat basophilic leukaemia cells (RBL-1) assay was applied to detect the LTB_4 secretion by ELISA (*40*, *48*). In comparison with these methods, our SPR-based screening assay for 5-LOX inhibitors avoids the troublesome and ethical problems of collecting whole human blood as material, and appears convenient and time-saving in not involving multiple steps like ELISA. SPR also showed no lower sensitivity and specificity than RIA or ELISA.

In summary, the current work employed SPR technology–based Biacore 3000 and molecular docking simulation analyses to study the binding features of seven 5-LOX inhibitors to human 5-LOX. The equilibrium dissociation constant (K_D) values evaluated by Biacore 3000 for the inhibitor binding to 5-LOX showed a good correlation with its reported IC_{50}, which suggests that SPR might be used as a direct assay method for screening new 5-LOX inhibitors at an early stage. Molecular docking technology was performed with the 3D structural model of 5-LOX generated on the basis of the crystal structure of rabbit reticulocyte 15-lipoxygenase, which has helped to investigate the 5-LOX/inhibitor binding at the atomic level. The fact that the predicted binding free energies for the inhibitors showed a good correlation with the K_D values measured by SPR assay and the reported IC_{50} implies the correctness of our constructed 3D structural model of 5-LOX. Our work will hopefully find application in the platform construction for structure-based 5-LOX inhibitor discovery.

This work was supported by the State Key Program of Basic Research of China (grants 2002CB512807, 2004CB58905), the National Natural Science Foundation of China (grants 30525024, 20472095), and the Shanghai Basic Research Project from the Shanghai Science and Technology Commission (grants 03DZ19228 and 03DZ19212).

REFERENCES

1. Ford-Hutchinson, A.W., Gresser, M., and Young, R.N. (1994) 5-Lipoxygenase. *Annu. Rev. Biochem.* **63**, 383–417
2. Samuelsson, B., Dahlen, S.E., Lindgren, J.A., Rouzer, C.A., and Serhan, C.N. (1987) Leukotrienes and lipoxins: structures, biosynthesis, and biological effects. *Science* **237**, 1171–1176
3. Shimizu, T., Radmark, O., and Samuelsson, B. (1984) Enzyme with dual lipoxygenase activities catalyzes leukotriene A4 synthesis from arachidonic acid. *Proc. Natl. Acad. Sci. USA* **81**, 689–693
4. Rouzer, C.A., Matsumoto, T., and Samuelsson, B. (1986) Single protein from human leukocytes possesses 5-lipoxygenase and leukotriene A4 synthase activities. *Proc. Natl. Acad. Sci. USA* **83**, 857–861
5. Samuelsson, B. (1983) Leukotrienes: mediators of immediate hypersensitivity reactions and inflammation. *Science* **220**, 568–575
6. Hay, D.W., Torphy, T.J., and Undem, B.J. (1995) Cysteinyl leukotrienes in asthma: old mediators up to new tricks. *Trends. Pharmacol. Sci.* **16**, 304–309
7. Shureiqi, I. and Lippman, S.M. (2001) Lipoxygenase modulation to reverse carcinogenesis. *Cancer. Res.* **61**, 6307–6312
8. Rioux, N. and Castonguay, A. (1998) Inhibitors of lipoxygenase: a new class of cancer chemopreventive agents. *Carcinogenesis* **19**, 1393–1400
9. Steele, V.E., Holmes, C.A., Hawk, E.T., Kopelovich, L., Lubet, R.A., Crowell, J.A., Sigman, C.C., and Kelloff, G.J. (1999) Lipoxygenase inhibitors as potential cancer chemopreventives. *Cancer. Epidemiol. Biomarkers. Prev.* **8**, 467–483
10. Lewis, R.A., Austen, K.F., and Soberman, R.J. (1990) Leukotrienes and other products of the 5-lipoxygenase pathway. Biochemistry and relation to pathobiology in human diseases. *N. Engl. J. Med.* **323**, 645–655
11. Jakobsson, P.J., Steinhilber, D., Odlander, B., Radmark, O., Claesson, H.E., and Samuelsson, B. (1992) On the expression and regulation of 5-lipoxygenase in human lymphocytes. *Proc. Natl. Acad. Sci. USA* **89**, 3521–3525
12. Balcarek, J.M., Theisen, T.W., Cook, M.N., Varrichio, A., Hwang, S.M., Strohsacker, M.W., and Crooke, S.T. (1988) Isolation and characterization of a cDNA clone encoding rat 5-lipoxygenase. *J. Biol. Chem.* **263**, 13937–13941
13. Skrzypczak-Jankun, E., Amzel, L.M., Kroa, B.A., and Funk, M.O., Jr. (1997) Structure of soybean lipoxygenase L3 and a comparison with its L1 isoenzyme. *Proteins* **29**, 15–31
14. Gillmor, S.A., Villasenor, A., Fletterick, R., Sigal, E., and Browner, M.F. (1997) The structure of mammalian 15-lipoxygenase reveals similarity to the lipases and the determinants of substrate specificity. *Nat. Struct. Biol.* **4**, 1003–1009
15. Borngraber, S., Browner, M., Gillmor, S., Gerth, C., Anton, M., Fletterick, R., and Kuhn, H. (1999) Shape and specificity in mammalian 15-lipoxygenase active site. The functional interplay of sequence determinants for the reaction specificity. *J. Biol. Chem.* **274**, 37345–37350
16. Hammarberg, T., Provost, P., Persson, B., and Radmark, O. (2000) The N-terminal domain of 5-lipoxygenase binds calcium and mediates calcium stimulation of enzyme activity. *J. Biol. Chem.* **275**, 38787–38793
17. McMillan, R.M. and Walker, E.R. (1992) Designing therapeutically effective 5-lipoxygenase inhibitors. *Trends. Pharmacol. Sci.* **13**, 323–330
18. Jelemont, F., Dogne, J.M., Laeckmann, D., Pirotte, B., and Leval, X. (2003) Recent developments of 5-LOX inhibitors. *Expert. Opin. Ther. Patents.* **13**, 1–13
19. Drazen, J.M., Israel, E., and O'Byrne, P.M. (1999) Treatment of asthma with drugs modifying the leukotriene pathway. *N. Engl. J. Med.* **340**, 197–206
20. Brain, S.D. and Williams, T.J. (1990) Leukotrienes and inflammation. *Pharmacol. Ther.* **46**, 57–66
21. Yu, C., Chen, L., Luo, H., Chen, J., Cheng, F., Gui, C., Zhang, R., Shen, J., Chen, K., Jiang, H., and Shen, X. (2004) Binding analyses between Human PPARgamma-LBD and ligands. *Eur. J. Biochem.* **271**, 386–397
22. Zhang, Y.Y., Radmark, O., and Samuelsson, B. (1992) Mutagenesis of some conserved residues in human 5-lipoxygenase: effects on enzyme activity. *Proc. Natl. Acad. Sci. USA* **89**, 485–489
23. Rich, R.L., Day, Y.S., Morton, T.A., and Myszka, D.G. (2001) High-resolution and high-throughput protocols for measuring drug/human serum albumin interactions using BIACORE. *Anal. Biochem.* **296**, 197–207

24. *Sybyl version 6.8* (2001) Tripos Associates, St. Louis, MO
25. Vinter, J.G., Davis, V.A., and Saunders, M.R. (1997) Strategic approaches to drug design. I. An intergrated software framework for molecular modeling. *J. Comput. Aided Mol. Des.* **1**, 31–51
26. Marsili, M. and Gasteiger, J. (1980) Pi-charge distributions from molecular topology and pi-orbital electronegativity. *Croat. Chem. Acta* **53**, 601–614
27. Gasteiger, J. and Marsili, M. (1980) Iterative partial equalization of orbital electronegativity—A rapid access to atomic charges. *Tetrahedron* **36**, 3219–3228
28. Greer, J. (1981) Comparative model-building of the mammalian serine proteases. *J. Mol. Biol.* **153**, 1027–1042
29. *Profiles-3D UserGuide* (1998) Molecular Simulations Inc.,San Diego
30. Laskonski, R.A., MacArthur, M.W., Moss, D.S., and Thornton, J.M. (1993) PROCHECK: A program to check the stereochemical quality of protein structures. *J. Appl. Crystallogr.* **26**, 283–291
31. Schwarz, K., Walther, M., Anton, M., Gerth, C., Feussner, I., and Kuhn, H. (2001) Structural basis for lipoxygenase specificity conversion of the human leukocyte 5-lipoxygenase to a 15-lipoxygenating enzyme species by site-directed mutagenesis. *J. Biol. Chem.* **276**, 773–779
32. Morris, G.M., Goodsell, D.S., Huey, R., Hart, W.E., Halliday, S., Belew, R.K., and Olson, A.J. (1998) Automated docking using a lamarchian genetic algorithm and empirical binding free energy function. *J. Comp. Chem.* **19**
33. Baba, A., Kimoto, M., Tatsuno, T., Inoue, T., and Iwata, H. (1985) Membrane-bound lipoxygenase of rat cerebral microvessels. *Biochem. Biophys. Res. Commun.* **127**, 283–288
34. Cho, H., Ueda, M., Tamaoka, M., Hamaguchi, M., Aisaka, K., Kiso, Y., Inoue, T., Ogino, R., Tatsuoka, T., Ishihara, T. *et al.* (1991) Novel caffeic acid derivatives: extremely potent inhibitors of 12-lipoxygenase. *J. Med. Chem.* **34**, 1503–1505
35. Neichi, T., Koshihara, Y., and Murota, S. (1983) Inhibitory effect of esculetin on 5-lipoxygenase and leukotriene biosynthesis. *Biochim. Biophys. Acta* **753**, 130–132
36. Yoshimoto, T., Yokoyama, C., Ochi, K., Yamamoto, S., Maki, Y., Ashida, Y., Terao, S., and Shiraishi, M. (1982) 2,3,5-Trimethyl-6-(12-hydroxy-5,10-dodecadiynyl)-1,4-benzoquinone (AA861), a selective inhibitor of the 5-lipoxygenase reaction and the biosynthesis of slow-reacting substance of anaphylaxis. *Biochim. Biophys. Acta* **713**, 470–473
37. Koshihara, Y., Neichi, T., Murota, S., Lao, A., Fujimoto, Y., and Tatsuno, T. (1984) Caffeic acid is a selective inhibitor for leukotriene biosynthesis. *Biochim. Biophys. Acta* **792**, 92–97
38. Hope, W.C., Welton, A.F., Fiedler-Nagy, C., Batula-Bernardo, C., and Coffey, J.W. (1983) In vitro inhibition of the biosynthesis of slow reacting substance of anaphylaxis (SRS-A) and lipoxygenase activity by quercetin. *Biochem. Pharmacol.* **32**, 367–371
39. Salari, H., Braquet, P., and Borgeat, P. (1984) Comparative effects of indomethacin, acetylenic acids, 15-HETE, nordihydroguaiaretic acid and BW755C on the metabolism of arachidonic acid in human leukocytes and platelets. *Prostaglandins. Leukot. Med.* **13**, 53–60
40. Hamasaki, Y. and Tai, H.H. (1985) Gossypol, a potent inhibitor of arachidonate 5- and 12-lipoxygenases. *Biochim. Biophys. Acta* **834**, 37–41
41. Thompson, J.D., Higgins, D.G., and Gibson, T.J. (1994) CLUSTAL W: improving the sensitivity of progressive multiple sequence alignment through sequence weighting, position-specific gap penalties and weight matrix choice. *Nucleic Acids Res.* **22**, 4673–4680
42. MacDonal, I.K. and Thornton, J.M. (1994) Satisfying hydrogen bonding potential in proteins. *J. Mol. Biol.* **238**, 777–793
43. Wallace, A.C., Laskouski, R.A., and Thornton, J.M. (1995) LIGPLOT: a program to generate schematic diagrams of protein-ligand interactions. *Protein Eng.* **8**, 127–134
44. Hammarberg, T. and Radmark, O. (1999) 5-lipoxygenase binds calcium. *Biochemistry* **38**, 4441–4447
45. Ueda, N., Kaneko, S., Yoshimoto, T., and Yamamoto, S. (1986) Purification of arachidonate 5-lipoxygenase from porcine leukocytes and its reactivity with hydroperoxyeicosatetraenoic acids. *J. Biol. Chem.* **261**, 7982–7988
46. Jakschik, B.A., Sun, F.F., Lee, L., and Steinhoff, M.M. (1980) Calcium stimulation of a novel lipoxygenase. *Biochem. Biophys. Res. Commun.* **95**, 103–110
47. Tavares, I.A. and Bennett, A. (1993) Acemetacin and indomethacin: differential inhibition of constitutive and inducible cyclo-oxygenases in human gastric mucosa and leucocytes. *Int. J. Tissue. React.* **15**, 49–53
48. Tries, S., Neupert, W., and Laufer, S. (2002) The mechanism of action of the new anti-inflammatory compound ML3000: inhibition of 5-LOX and COX-1/2. *Inflamm. Res.* **51**, 135–143